Journal of Applied Mechanical Engineering
ISSN: 2168-9873

Zheng and Wang, J Appl Mech Eng 2016, 5:1
DOI: 10.4172/2168-9873.1000194

Research Article Open Access

Fourier Analysis of Milling Force for General Helical Cutters via Space-time Convolution, Part 1: Model Development

Zheng CM[1]* and Junz Wang JJ[2]

[1]Department of Mechanical and Electrical Engineering, Quanzhou Institute of Information Engineering, Quanzhou 36200, PR China
[2]Department of Mechanical Engineering, Department of Mechanical Engineering, National Cheng Kung University, Tainan, Taiwan(R.O.C) 701 01, PR China

Abstract

A space-time convolution approach to analyze the milling force for a general helical cutter is proposed. The single flute cutting force is firstly established through an integrated space-time convolution process. Subsequently, multi-flute milling forces are obtained through convolution integration in time domain (*i.e.*, angular domain). In this convolution force model, convolution theorem does not apply directly and a modified convolution theorem is presented to find the Fourier coefficients of the total milling force for any analytically definable helical cutter. From the Fourier analysis, the magnitudes of higher order Fourier coefficients are shown to drop off quickly. Therefore, the capability to extract a small number of Fourier coefficients as characteristic values of milling forces is an important advantage of this convolution force model. Furthermore, this model provides a convenient means to calculate the Fourier coefficients of the milling forces if the profile of cutter/workpiece can not be analytically definable and only the discrete values of cutter/workpiece profile data are given from scanning. Also, the general effects of cutter geometry and cutting parameters on the spectra characteristics of the milling forces are extracted and discussed. Based on the spectra characteristics, the strategy of selecting cutters for rough and finish machining in slot milling is presented.

Keywords: Fourier coefficients; Force model; Space-time convolution; Modified convolution theorem; General helical cutter

Nomenclature

A	Fourier series coefficient of the total forces
α, α_o	helix angle along the cutting edge and nominal helix angle
β	radial angular position of cutting point on the cutter
β_1, β_2,	lower and upper limits of radial engagement of the cutter
β_a, β_p	radial angle of axial immersion and flute spacing angle
C	workpiece offset
da, dr	axial and radial cutting depth
df, dfx, dfy, dfz	differential cutting forces in vector form and its components.
dft, dfr, dfa	differential local cutting forces in tangential, radial and axial directions
φ	cutter angular displacement
f1, F1	cutting force vector of the first flute, Fourier transform of f1
h, $h1$, $h2$	axial position of cutting point, lower and upper limits of axial depth
$h'(\beta)$, $h_w'(\beta)$	helix lead and chip width density functions
k_{ts}, k_{rs}, k_{as}	Shearing force constants in tangential, radial and axial directions
k_{tp}, k_{rp}, k_{ap}	ploughing force constants in tangential, radial and axial directions
N	number of cutter flutes
p1, p2	elemental force vectors due to shearing and ploughing mechanisms
p1w, p2w	windowed p1 and p2 functions
P1w, P2w	Fourier transforms of p1w and p2w
q1, q2	directional matrices for the shearing and ploughing forces
θ	angular position of cutting point in the work
R, Ro	radius function of cutting point on the cutter and nominal radius
T	transfer matrix between the measured cutting forces and cutting constants
t_c, t_x	uncut chip thickness and feed per tooth
wr(θ, h), wa(β)	radial and axial cutting window functions
ω	normalized frequency with respect to the spindle frequency
ψ,ψa	slope angle of cutting point and axial immersion angle

***Corresponding author:** Zheng CM, Department of Mechanical and Electrical Engineering, Quanzhou Institute of Information Engineering, Quanzhou 36200, PR China, Tel: 1-86-595-22765; E-mail: cmzheng1206@gmail.com

Received December 21, 2015; **Accepted** January 21, 2016; **Published** January 23, 2016

Citation: Zheng CM, Junz Wang JJ (2016) Fourier Analysis of Milling Force for General Helical Cutters via Space-time Convolution, Part 1: Model Development. J Appl Mech Eng 5: 194. doi:10.4172/2168-9873.1000194

Introduction

Milling force directly reflects work material properties, tool geometry, and any variation in the cutting conditions and thus carries rich information about the milling process. On the other hand, it is directly or indirectly responsible for many undesired phenomena such as vibration, dimensional error and tool wear. Hence, a great deal of research has been devoted to the investigation of milling force and creating milling force models [1,2]. Two key elements have to be considered in establishing a milling force model: defining a local force model and devising an integration process to compose the total forces from the local forces contributed by all the engaging cutting elements. While the integration process determines the efficiency and versatility of the milling force model, the effectiveness of the milling force model hinges upon the accuracy of the chosen local force model. An empirical local force model was first proposed by Koenigsberger and Sabberwal [3], in which a tangential force is related to the uncut chip thickness by a specific cutting coefficient. Similarly, Tlusty et al. [4] proposed using a radial cutting constant that relates the radial force to the uncut chip thickness. Both the tangential and radial cutting coefficients vary with the chip thickness and increase significantly as the uncut chip thickness becomes very small, which is often called the size effect. Boothroyd [5] suggested the use of an additional ploughing force in explaining the size effect. It is thought the constant ploughing force becomes a greater proportion of the total cutting force as the chip thickness decreases and therefore results in high specific cutting coefficients. Although the ploughing force has been early recognized [6], it is often not separately considered in the milling force model, but rather is combined with the chip removal force to become a lumped force model. In contrast, the dual-mechanism force model explicitly and separately considers the effects of the ploughing and shearing mechanisms in the cutting process. Yellowley [7] first proposed the separate use of a cutting force for the chip shearing and a parasitic force for the edge ploughing effect in the milling force model. Both the shearing and ploughing cutting coefficients were assumed to be constant and independent of the chip thickness. Armarego et al. [8] also used the dual-mechanism model and suggested that the shearing and ploughing coefficients be expressed as functions of tool edge geometry and cutting mechanics dependent parameters. From the interference geometry of the tool edge, Endres et al. [9] modeled and validated a ploughing force model using empirical cutting coefficients in the proposed dual-mechanism force model. Budak et al. [10] showed that for general milling conditions the size effect can be ignored and the dual cutting coefficients can be assumed as constants.

Composing the total milling forces from the local forces can be achieved through numerical, analytical, or a combination of these two processes [11]. Numerical model affords great flexibility in considering dynamic chip load variation or complex cutting edge geometry including runout effect. Kline et al. [12] established an end milling force model through numerical integration of the local force with the lumped force model. This numerical force model has served as the basic framework for many other milling force models developed afterwards.

A great percentage of the milling cutters in use today belong to the family of helical milling cutters including the typical square, conical, bull-nose and ball-end mills. Although their appearances and intended applications vary, they do share many common geometric features and in that respect a system of designation has been specified in the DIN66215 standard. The fact that these cutters possess similar geometric features suggests that a generalized force model can and should be developed in a unified framework to accommodate this family of cutters. Altintas and Lee [13] are the first to present a numerical force model for a cutter with general cutting edge profile including ball end mill with a fixed helix lead and taper end mill with a constant helix angle. Engin and Altintas [14] enhance this force model by adding other types of end mills including: bull nose, cone, rounded, inverted cone, and taper ball end mills. Wan et al. [15] developed a numerical force model for general end mills including runout effect using lumped shearing cutting coefficients. Based on the motion analysis, Sun and Guo [16] proposed a numerical force model for general end mills considering runout effect to predict cutting force in five-axis milling process.

On the other hand, analytical models generally yield more efficient computation and allow deeper insights into the effects of various cutting parameters on the milling force characteristics. Yellowley [17] derived Fourier series expressions for the torque and forces of a single tooth and showed that the quasi-mean resultant force was directly proportional to the magnitude of the fundamental frequency of torque for a single flute cutter. The Fourier coefficients and the force to torque ratio were utilized in ref. [18] to track the immersion angle and tool wear. For a face milling cutter, Seethaler and Yellowley [19] further derived the Fourier series coefficients of the offset related force for the identification of radial runout. However, the analytical models in ref. [17-19] are not applicable for a multi-flute helical cutter since these Fourier series expressions did not include the concurrent effect of both helix angle and multiple cutting teeth.

Based on the convolution integration concept, an analytical force model for end milling process was established by Wang et al. [20]. The Fourier coefficients of the periodic milling force were expressed as an explicit algebraic equation in terms of depths of cut and cutter geometry including helix angle, diameter and number of flutes. Zheng et al. [21] extended the convolution concept in a general force model for face milling and end milling processes. Using the same convolution approach, Lazoglu and Liang [22] presented a force model for the ball end milling process where an analytical expression is obtained under specific cutting conditions. These convolution force models in ref. [20-22] all use lumped cutting constants and are only applicable for one type of cutter. Based on the dual-mechanism model, Wang and Zheng established an analytical force model for a square end mill [23], and in ref. [24], a formula was derived for the identification of five cutting constants for the ball-end milling process using the average forces from one slot and one half slot milling processes. However, previous convolution force models for milling process are only applicable for the cutting condition with fixed radial cutting window where entry and exit cutting angles are limited to be constant.

By combining the modified convolution theorem presented in this study and the application of differential geometry and Fourier transform, a dual-mechanism frequency domain force model is herein proposed for a general helical cutter with variable radial cutting window, in which allowing entry and exit cutting angles vary with the axial position of the active cutting edge when convolution integration is performed to obtain Fourier coefficients of the total cutting force. The angle convolution and frequency decomposition of the milling forces is presented next. Section 3 analyzes the effects of the cutting parameters on the force spectra followed by conclusions for part 1 of this paper. Part 2 of this paper will continue with the application of this frequency domain force model for the common industrial cutters.

The Generalized Frequency Domain Force Model

Angle convolution of the differential forces

The geometries of a general helical cutter and the milling process

are defined through the work and cutter coordinates shown in Figure 1. It is assumed that each cutting edge can be mathematically represented in the cylindrical R-β-h coordinate. The angular position of the cutter is positioned so that the bottom of an arbitrarily chosen first flute at β $=h=0$ is located at $\theta=0$ when the angular displacement of the cutter φ is zero. It is therefore evident that $\theta=\varphi-\beta$. The general geometry of the first curvilinear cutting edge can be defined by two constraint equations:

$$R = R(h) \quad \text{and} \quad h = h(\beta)$$

The first equation determines the external profile or the surface envelope of the helical cutter and the second one defines the helical lead of the cutting edge on the profile surface. The elevation angle ψ of a cutting point is referred to as the intersecting angle between the cutter axis and its normal of the generatrix curve of the external profile as shown in Figure 1.

The three components of the differential local force, df_t, df_r and df_a, are represented in six cutting constants and expressed in the following linear vector form:

$$\begin{pmatrix} df_t \\ df_r \\ df_a \end{pmatrix} = \begin{pmatrix} 1 \\ k_{rs} \\ k_{as} \end{pmatrix} k_{ts} t_c db + \begin{pmatrix} 1 \\ k_{rp} \\ k_{ap} \end{pmatrix} k_{tp} db$$

$$\text{where } t_c = t_x \sin\theta \sin\psi \text{ and } db = \frac{dh}{\sin\psi}$$

k_{ts}, k_{rs}, and k_{as} in Eq. (2) represent the specific shearing constants for the chip removal force acting in the tangential, radial, and axial directions respectively; k_{tp}, k_{rp}, and k_{ap}, are the ploughing counterparts as shown by their subscripts. For a cutting point located at ψ on the cutter and at θ in the work, this differential local cutting force can also be expressed in the X-Y-Z coordinate:

$$d\mathbf{f} = \begin{pmatrix} df_x \\ df_y \\ df_z \end{pmatrix} = \begin{bmatrix} \cos\theta & \sin\psi\sin\theta & \cos\psi\sin\theta \\ \sin\theta & -\sin\psi\cos\theta & -\cos\psi\cos\theta \\ 0 & \cos\psi & -\sin\psi \end{bmatrix} \begin{pmatrix} df_t \\ df_r \\ df_a \end{pmatrix}$$

Substituting Eq. (3) into (2) results in the following expression for the local force per unit chip width:

$$\frac{\mathbf{df}}{dh} = \sum_{i=1}^{2} \mathbf{q}_i(\psi)\mathbf{p}_i(\theta, h)$$

where

$$\mathbf{p}_1(\theta) = k_{ts} t_x \begin{pmatrix} p_1(\theta) \\ p_2(\theta) \\ p_3(\theta) \end{pmatrix} = k_{ts} t_x \begin{pmatrix} \sin\theta\cos\theta \\ \sin^2\theta \\ \sin\theta \end{pmatrix} \quad \text{and}$$

$$\mathbf{p}_2(\theta) = k_{tp} \begin{pmatrix} p_4(\theta) \\ p_5(\theta) \\ p_6(\theta) \end{pmatrix} = k_{tp} \begin{pmatrix} \cos\theta \\ \sin\theta \\ 1 \end{pmatrix} \tag{5b}$$

$$\mathbf{q}_1(\psi) = \begin{bmatrix} 1 & k_{rs}\sin\psi + k_{as}\cos\psi & 0 \\ -(k_{rs}\sin\psi + k_{as}\cos\psi) & 1 & 0 \\ 0 & 0 & k_{rs}\cos\psi - k_{as}\sin\psi \end{bmatrix}$$

$$\mathbf{q}_2(\psi) = \begin{bmatrix} \frac{1}{\sin\psi} & (k_{rp} + k_{ap}\cot\psi) & 0 \\ -(k_{rp} + k_{ap}\cot\psi) & \frac{1}{\sin\psi} & 0 \\ 0 & 0 & (k_{rp}\cot\psi - k_{ap}) \end{bmatrix} \tag{6b}$$

$\mathbf{p}_1$ and $\mathbf{p}_2$ are the elemental force functions due to the shearing and the ploughing mechanisms respectively and physically represent the tangential force vectors per unit chip width in the X-Y-Z coordinate system. p_1-p_3 in Eq. (5) are shown to differ from p_4-p_6 in Eq. (5b) by a $\sin\theta$ term resulting from the inclusion of chip thickness in the shearing force component. The $\mathbf{q}_1$ and $\mathbf{q}_2$ are the directional matrices for the shearing and ploughing respectively. They transform the local forces to the X-Y-Z coordinate system and reflect the influence of elevation angle, ψ, along with radial and axial cutting constants on the magnitude and direction of the local cutting forces. A unit cutting window function $w_r(\theta, h)$ should be included in Eq. (5) to represent the radial cutting range in the work between the entry angle, θ_1, and exit angle, θ_2, which are determined by, the workpiece offset, c, the cutter radius and the radial depth of cut at the axial position, h, of a cutting point, that is

$$\theta_1(h) = \cos^{-1}\left(1 - \frac{c(h)}{R(h)}\right) \quad \text{and} \quad \theta_2(h) = \cos^{-1}\left(1 - \frac{c(h) + d_r(h)}{R(h)}\right)$$

The radial cutting window function is defined by

$$w_r(\theta, h) = \begin{cases} 1 & \text{when } \theta \in [\theta_1(h), \theta_2(h)] \\ 0 & \text{otherwise} \end{cases}$$

Note that the radial cutting window function $w_r(\theta, h)$ presented here is a variable cutting window which is related to the axial position of active cutting edge, and the variable cutting window can be a fixed cutting window $w_r(\theta)$ in slot and half slot milling for a general helical mill. The cutting force generated by the first tooth of the cutter then can be obtained by integrating d**f** over the axial depth of cut and, with a change of variable, is given by

$$\mathbf{f}_1(\phi) = \int_{h_1}^{h_2} \frac{d\mathbf{f}(\psi, \theta)}{dh} dh = \sum_{i=1}^{2} \int_{h_1}^{h_2} \mathbf{q}_i(\psi)\mathbf{p}_i(\theta) w_r(\theta, h) dh = \sum_{i=1}^{2} \int_{\beta_1}^{\beta_2} \mathbf{q}_i(\psi)\mathbf{p}_{iw}(\theta, h) h'(\beta) d\beta$$

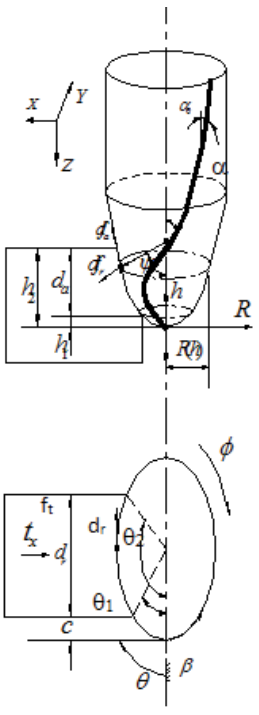

Figure 1: Coordinate systems for the milling process and geometry of a general helical cutter.

where $\mathbf{p}_{iw}(\theta,h)=\mathbf{p}_i(\theta)w_r(\theta,h)$

is the windowed function of $\mathbf{p}_i(\theta)$ and $h'(\beta)\,d\beta$ replaces dh in the last equality. β_1 and β_2 in Eq. (9) are the lower and upper limits of radial engaging range on the cutter corresponding to the lower and upper limits of axial depth of cut at h_1 and h_2 as shown in Figure 1. $h'(\beta)$ is the derivative of the axial position function, $h(\beta)$, and geometrically represents the helix lead at β. In the context of the force integration, $h'(\beta)$ represents the differential chip width per differential radial immersion angle of the cutter. Based on $h'(\beta)$, a chip width density function, $h_w'(\beta)$, can be defined for the milling process by multiplying a unit axial cutting window, $w_a(\beta)$, to reflect the effect of axial depth of cut; that is

$$h_w'(\beta)=h'(\beta)w_a(\beta)$$

where

$$w_a(\beta)=\begin{cases}1 & \text{when } \beta\in[\beta_1(h),\beta_2(h)]\\ 0 & \text{otherwise}\end{cases}$$

It is noted that $w_a(\beta)$ is a fixed cutting window since β_1 and β_2 are specified values in milling.

Similar to the relationship between $\mathbf{p}_{iw}(\theta)$ and $\mathbf{p}_i(\theta)$, the chip width density function $h_w'(\beta)$ is a windowed function of $h'(\beta)$ and is the same as the helical lead function except that it is bounded by the lower and upper axial cutting limits, β_1 and β_2 Note that ψ and h are functions of β defined by the curvilinear edge geometry of the general helical cutter and hence $\mathbf{q}_i(\psi(\beta))$ and $\mathrm{p}_{1w}(,h(\beta))$ are also functions of β. With a change of variables and substitution of Eq. (11) and $\theta=\varphi-\beta$, Eq. (9) can be rewritten as

$$\mathbf{f}_1(\phi)=\sum_{i=1}^{2}\int_{-\infty}^{\infty}\mathbf{q}_i(\beta)\mathbf{p}_{iw}(\phi-\beta,h)dh$$

$$=\sum_{i=1}^{2}\int_{-\infty}^{\infty}h_w'(\beta)\mathbf{q}_i(\beta)\mathbf{p}_{iw}(\phi-\beta,\beta)d\beta=\left[\sum_{i=1}^{2}(h_w'\cdot\mathbf{q}_i)*\mathbf{p}_{iw}\right](\phi)$$

where * denotes the convolution operation and the integration limits in Eq. (9) are implicitly embedded in the chip width density function, $h_w'(\beta)$. Since the variable cutting window $w_r(\theta, h)$ is related to the axial position of active cutting edge as mentioned early, the $\mathbf{p}_{iw}$ in Eq. (13) is defined over space h as well as time φ/ϖ (ϖ = spindle speed in rad/s). The processing of force signals in Eq. (13) therefore is an integrated space-time convolution process as shown in Figure 2. In Figure 2(a), one could image that two controllers are used to adjust the entry and exit positions of the variable cutting window, respectively, and the entry and exit positions depend on the axial position of the cutting element, $h(\beta)$. The cutting force generated by the first tooth of the cutter then can be modeled as the summation of the space-time convolutions at each axial position as shown in Figure 2(b). Therefore, it is necessary to consider the relative effect of axial position of the cutting element on the convolution process in time domain or angular domain. Eq. (13) also shows that the local shearing force functions, $\mathbf{q}_1$ and $\mathbf{p}_{1w}$, and the local ploughing force functions, $\mathbf{q}_2$ and $\mathbf{p}_{2w}$, contribute to the total forces through the same convolution structure. They differ in their respective cutting constants and the additional chip thickness term in the tangential shearing force vector, $\mathbf{p}_{1w}$.

Gygax [25] first brought up the concept of convolution for extending the single-tooth face milling force to multi-tooth face milling forces without, however, providing a specific formulation. Wang et al. [21] proposed a periodic tooth sequence function $ts(\varphi)$ to represent the rotating multi-flute cutter as an input function to convolve with the single tooth cutting forces, $\mathbf{f}_1(\varphi)$, with the resulting convolution integral being the total milling forces of the multi-flute cutter, $\mathbf{f}(\varphi)$ as shown in Figure 3. In mathematic expression,

$$ts(\phi)=\sum_{k=-\infty}\delta(\phi-(k-1)\beta_p)$$

with

$$ts(\phi)=\sum_{k=-\infty}^{\infty}\delta(\phi-(k-1)\beta_p)$$

where the index k indicates the kth flute of the cutter and β_p is the angle between uniformly spaced flutes. Equation (14) indicates that the total milling forces are in fact the sums of the periodically shifted first flute forces corresponding to the consecutive cutting action of the rotating cutter. It is evident that the total milling force in Eq. (14) is periodic and this suggests that a Fourier series representation in the frequency domain would be more efficient and suitable for computation and analysis of the milling forces.

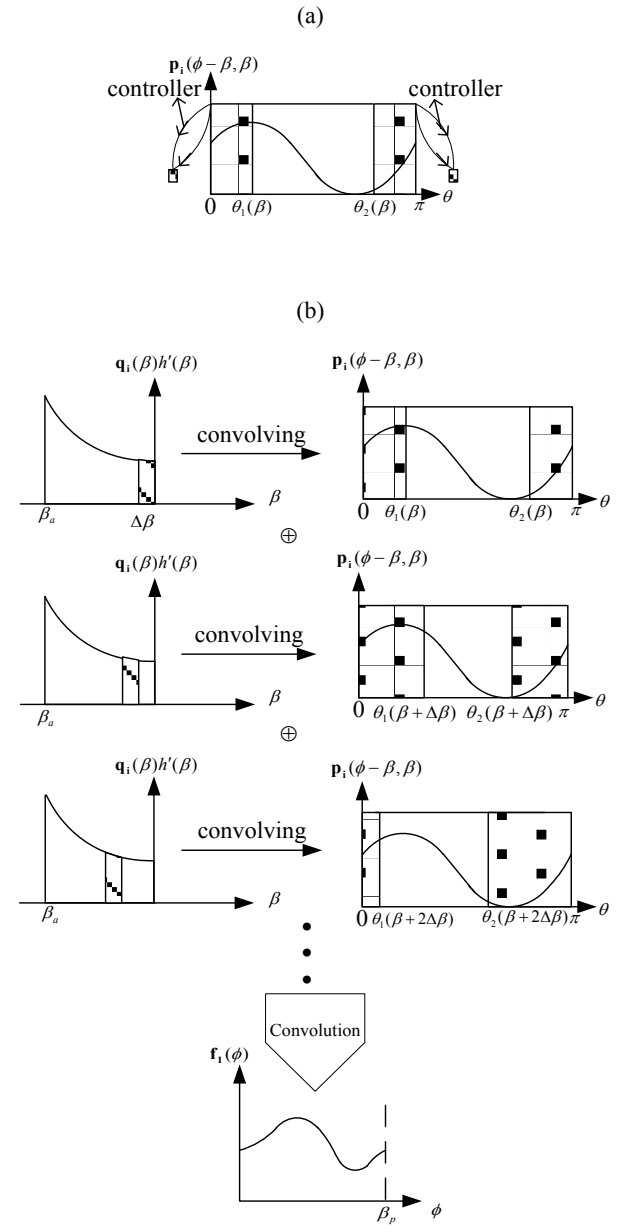

Figure 2: (a): Variable cutting window. (b): Space-time convolution process of single flute cutting force.

Analytical integral expression of the Fourier coefficients of total milling forces

Fourier series expansion of the total force in Eq. (14) can be shown to be

$$\mathbf{f}(\phi)=\sum_{k=-\infty}^{\infty}\mathbf{A}[Nk]e^{jNk\phi}\quad\text{where}\quad\mathbf{A}[Nk]=\begin{pmatrix}A_x[Nk]\\A_y[Nk]\\A_z[Nk]\end{pmatrix}=\frac{N}{2\pi}\mathbf{F}_1(NK)$$

$\mathbf{A}[Nk]$ are the Fourier coefficients for the kth harmonic of the total cutting forces and represent the magnitudes and phases of cutting force components at the normalized, $\omega = Nk$. $\mathbf{F}_1(Nk)$ is the Fourier transform of $\mathbf{f}_1(\varphi)$, $\mathbf{F}_1(\omega)$, evaluated at $\omega = Nk$. It should be noted that $\mathbf{f}_1(\varphi)$ in Eq. (13) is modeled as an integrated space-time convolution process as mentioned early and then $\mathbf{F}_1(\omega)$ can not be found directly from $\mathbf{f}_1(\varphi)$ by convolution theorem because convolution theorem can only do with the transform in time domain or space domain. Discussion described above suggests that a modified convolution theorem should be established to convert $\mathbf{f}_1(\varphi)$ into $\mathbf{F}_1(\omega)$. To do this, $\mathbf{F}_1(\omega)$ can be obtained as shown in the following:

$$\mathbf{F}_1(\omega)=\int_{-\infty}^{\infty}\mathbf{f}_1(\phi)e^{-j\omega\phi}d\phi=\int_{-\infty}^{\infty}\left\{\sum_{i=1}^{2}\int_{-\infty}^{\infty}h'_w(\beta)\mathbf{q}_i(\beta)\mathbf{p}_{iw}(\phi-\beta,\beta)d\beta\right\}e^{-j\omega\phi}d\phi$$
$$=\sum_{i=1}^{2}\int_{-\infty}^{\infty}\left\{\int_{-\infty}^{\infty}h'_w(\beta)\mathbf{q}_i(\beta)\mathbf{p}_{iw}(\phi-\beta,\beta)e^{-j\omega\phi}d\phi\right\}d\beta$$
$$=\sum_{i=1}^{2}\int_{-\infty}^{\infty}h'_w(\beta)\mathbf{q}_i(\beta)\mathbf{P}_{iw}(\omega,\beta)e^{-j\omega\beta}d\beta=\sum_{i=1}^{2}\mathbf{F}_{1i}(\omega)$$

where the first line is by the Fourier transform definition. The sequence of integration is exchanged and the shifting property of the Fourier transform applied in the second line. In the third line, $\mathbf{F}_{1i}(\omega)$'s are the Fourier transforms of the shearing and ploughing force components of the first flute and $\mathbf{P}_{iw}(\omega,\beta)$'s is shown to be:

$$\mathbf{P}_{iw}(\omega,\beta)=\int_{-\infty}^{\infty}\mathbf{p}_{iw}(\phi,\beta)e^{-j\omega\phi}d\phi=\int_{\theta_1(\beta)}^{\theta_2(\beta)}\mathbf{p}_i(\theta,\beta)e^{-j\omega\theta}d\theta$$

Note that $\mathbf{P}_{iw}(\omega, \beta)$ is the Fourier transform of $\mathbf{p}_{iw}$ at the specified axial position $h(\beta)$ with respect to φ and does not represent global Fourier transform of $\mathbf{p}_{iw}$ over the cutting region. Carrying out the integration in Eq. (18) will have

$$\mathbf{P}_{1w}(\omega,\beta)=k_{te}t_z\begin{pmatrix}P_{1w}(\omega,\beta)\\P_{2w}(\omega,\beta)\\P_{3w}(\omega,\beta)\end{pmatrix}=k_{te}t_z\begin{pmatrix}\frac{e^{-j\omega\theta}}{2(\omega^2-4)}(j\omega\sin2\theta+2\cos2\theta)\\-\frac{e^{-j\omega\theta}}{2j\omega}-\frac{e^{-j\omega\theta}}{2(\omega^2-4)}(j\omega\cos2\theta-2\sin\theta)\\\frac{-e^{-j\omega\theta}}{1-\omega^2}(j\omega\sin\theta+\cos\theta)\end{pmatrix}_{\theta=\theta_1(\beta)}^{\theta_2(\beta)}\tag{19}$$

$$\mathbf{P}_{2w}(\omega,\beta)=k_{tp}\begin{pmatrix}P_{4w}(\omega,\beta)\\P_{5w}(\omega,\beta)\\P_{6w}(\omega,\beta)\end{pmatrix}=k_{tp}\begin{pmatrix}\frac{e^{-j\omega\theta}}{\omega^2-1}(j\omega\cos\theta-\sin\theta)\\\frac{e^{-j\omega\theta}}{\omega^2-1}(j\omega\sin\theta+\cos\theta)\\\frac{-e^{-j\omega\theta}}{j\omega}\end{pmatrix}_{\theta=\theta_1(\beta)}^{\theta_2(\beta)}\tag{19b}$$

The entry and the exit angles that define the radial cutting window in the angular domain have become the integration limits in Eqs. (19) and (19b).

As mentioned early, the variable cutting window function $w_r(\theta, h)$ can be a fixed cutting window function $w_r(\theta)$ in slot milling for a general helical mill and then the convolution process of $\mathbf{f}_1(\varphi)$ can be reduced from Figures 2-4. Namely, $\mathbf{P}_{iw}(\omega, \beta)$ can be simplified as $\mathbf{P}_{iw}(\omega)$. Substituting $\mathbf{P}_{iw}(\omega)$ into (17) results in the following expression:

$$\mathbf{F}_1(\omega)=\sum_{i=1}^{2}\mathbf{P}_{iw}(\omega)\int_{-\infty}^{\infty}h'_w(\beta)\mathbf{q}_i(\beta)e^{-j\omega\beta}d\beta=\sum_{i=1}^{2}\mathbf{P}_{iw}(\omega)\mathbf{Q}_{iw}(\omega)=\sum_{i=1}^{2}\mathbf{F}_{1i}(\omega)\tag{20}$$

where $\mathbf{Q}_{iw}(\omega)$ represents the Fourier transform of $h'_w.q_i$. Equation (20) shows that convolution theorem is applicable to obtain the Fourier

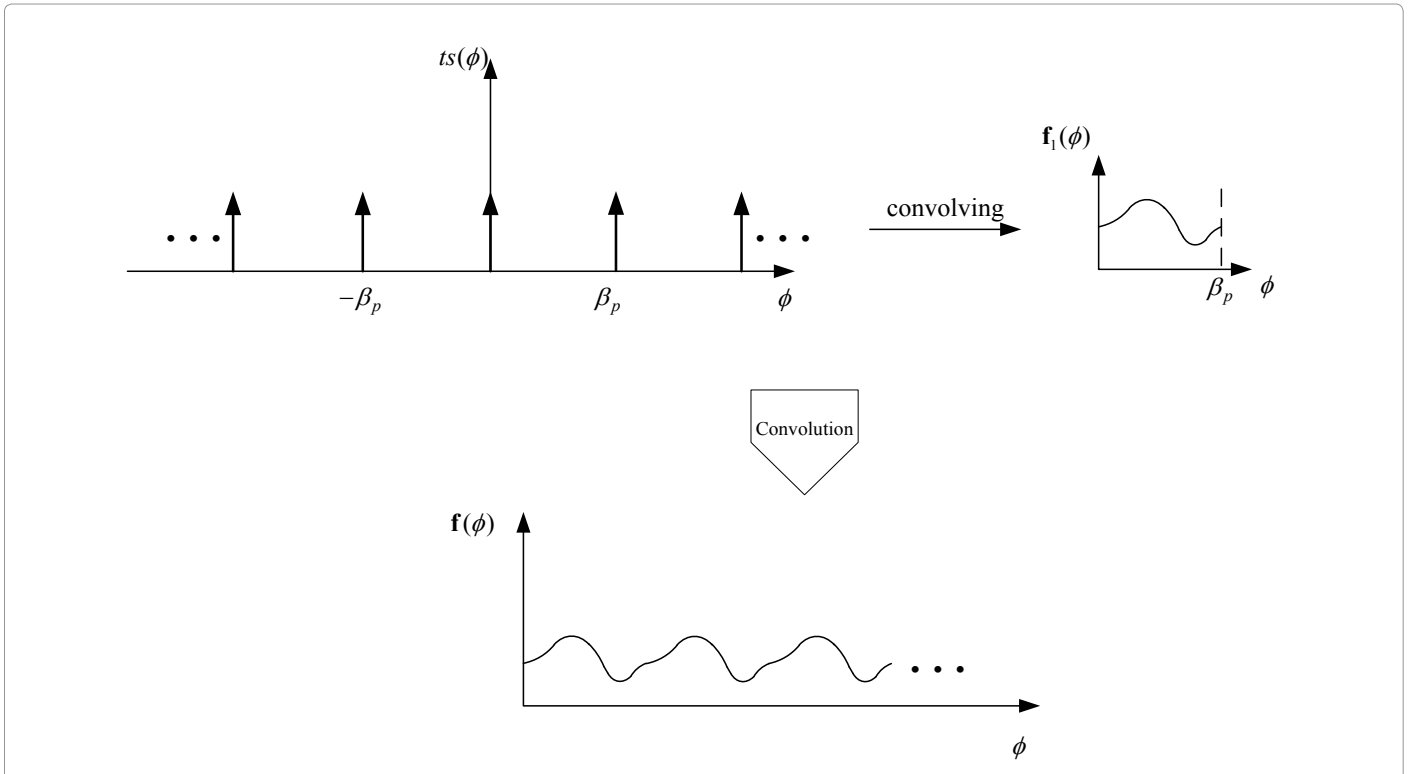

Figure 3: Convolution process of multi-flute milling force.

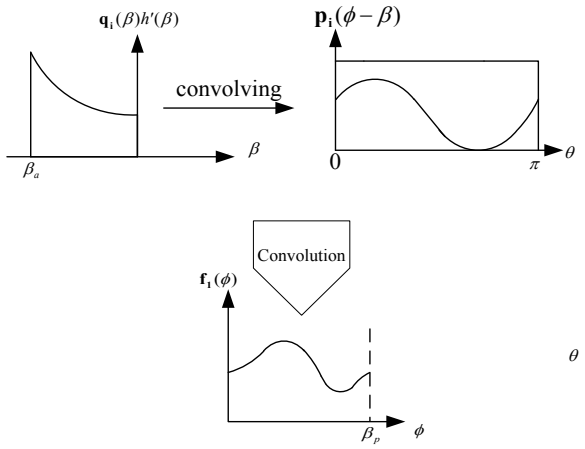

Figure 4: Convolution process of single flute cutting force for slot milling.

transform of $\mathbf{f}_1(\varphi)$ directly when radial cutting window function $w_r(\theta, h)$ is limited as a fixed cutting window function $w_r(\ )$. Also, expression of Eq. (17) is shown to be a modified convolution theorem which is able to accommodate convolution theorem.

Eq. (16) for the Fourier coefficients of the milling forces along with Eqs. (17-20) represent the frequency domain force model for a general helical end mill. Within these equations, the geometric and cutting parameters of a general milling process have been integrated into a unified analytical framework, thus allowing the effect of each individual parameter on the force characteristics to be investigated.

Spectra Analysis of the Milling Forces

The effects of mill geometry on frequency characteristics

In the angular domain, as in Eq. (14), the flute number determines the spacing of the shifted single flute forces. The larger N is, the closer the spacing and thus the multiple single flute forces superimpose and smear the individual force profile. In the frequency domain, as in Eq. (16), other than picking out the harmonic frequencies at $\omega = Nk$, the flute number has the multiplying effect of a factor N for all the harmonics as well as the average forces. In contrast to the spacing in the time domain, the larger N is, the farther apart the spacing of the harmonic frequencies becomes.

The Fourier coefficients of the kth harmonics of the total forces in Eq. (16) are obtained through Eq. (17) as the integration of the Fourier transform at $\omega=Nk$ of the differential cutting forces per unit radian engagement of the cutting edge in the circumferential coordinate,β. This Fourier transform of the differential force is shown to be the product of the cutter geometric functions in $\mathbf{q}_i(\psi(\beta))$ and $h'(\beta)$ and the frequency transform of the elemental cutting function, $\mathbf{P}_{iw}$. $\mathbf{P}_{iw}(Nk, \beta)$'s in Eqs. (19) and (19b) represent the contributions of shearing and ploughing tangential forces by the cutting point at β to the kth harmonic of the total cutting forces. Values of $\mathbf{P}_{iw}(\omega,\beta)$'s depend upon the entry and exit angles at β, $\theta_1(\beta)$ and $\theta_2(\beta)$ and are characterized by magnitude decay in ω^{-1}.

$\mathbf{q}_i(\psi(\beta))$ and $h_w'(\beta)$ are cutter geometry dependent. Having the same role as in the angular domain, $\mathbf{q}_i(\beta)$'s in Eqs. (6) and (6b) are the directional matrices which redirect and magnify the tangential shearing and ploughing vectors, $\mathbf{P}_{iw}(Nk, \beta)$'s. The chip width density function $h_w'(\beta)$ carries the weighting of helical lead at point β. For a cutter with a constant helix lead, the spectra of chip width density function have magnitude decay in ω^{-1} [20]. The combined frequency decay from $h_w'(\beta)\mathbf{P}_{iw}(Nk,\beta)$ therefore is in ω^{-2}. Considering the N factor in Eq. (13), it can be shown that the average forces are proportional to N while in most situations the kth harmonic components at $\omega = Nk$ is at most proportional to $(Nk)^{-1}$. This shows that in general dynamic component of the milling forces is reduced and more information would be lost in the milling forces as N increases with other cutting conditions remaining the same. This is equivalent to the smearing effect of the superimposed multi-flute forces in the angular domain and would explain why single tooth cutting is often preferred over multi-flute milling in the investigation of cutting process through milling forces. Due to this frequency decay, the magnitudes of higher order terms in Eq. (13) drop off quickly and only the first few terms will have significant values. Therefore, the milling forces in the continuous angular or time domain can be adequately represented by few numerical values in the discrete frequency domain. Its capability to extract a small number of characteristic values from forces of continuous time or angle domain is an important advantage of the frequency domain force model.

Equation (17) is evaluated by integrating over a cutting region in the β-θ plane with four boundaries defined by $\beta_1, \beta_2, \theta_1(\beta)$ and $\theta_2(\beta)$. The integration limits, β_1 and β_2, are the end points of the radial engagement of the cutter and are determined by the axial depth of cut as well as the cutter geometry, $h(\beta)$. The other pair of integration limits, $\theta_1(\beta)$ and $\theta_2(\beta)$, determine the Fourier transform of the elemental cutting forces in Eq. (18) for any cutting element between β_1 and β_2. They are the entry and exit angles determined by the radial depth of cut, $d_r(\beta)$, and cutter radius, $R(\beta)$. All these three functions, h', $\mathbf{q}_i$, $\mathbf{P}_{iw}$ and the integration boundaries in Eq. (17) explicitly or implicitly depend on the geometry of the cutting edge. The cutting edge geometry together with the axial and radial depths of cut thus completely characterizes the milling force spectra through Eq. (17).

While the geometric functions $\mathbf{q}$ and h' are completely dependent on the geometry of the helical cutter and will be discussed in the part 2 of this paper for some common cutters, the elemental force functions $\mathbf{P}_{iw}(\omega)$'s possess frequency characteristics which are independent of the cutter geometry and are common for a general helical cutter. This point along with other features of the $\mathbf{P}_{iw}(\omega)$ function will be analyzed next.

The effects of radial immersion on zeros of the frequency spectra

$\mathbf{P}_{iw}(\omega, \beta)$'s as in Eqs.(19-19b) are expressions for the Fourier transforms of the windowed elemental force functions $\mathbf{p}_i(\theta)w_r(\theta, \beta)$ at the specified axial poison $h(\beta)$ in a general cutting configuration. They are, however, not in a form amenable to examining the effect of radial cutting depth on the frequency spectra. They can be alternatively derived through the modulation property of the Fourier transform by expressing $\mathbf{P}_{iw}(\omega, \beta)$ as the convolution of $\mathbf{P}_i(\omega)$ and $W_r(\omega, \beta)$, the Fourier transforms of $\mathbf{p}_i(\theta)$ and $w_r(\theta, \beta)$, respectively [26], that is,

$$\mathbf{P}_{iw}(\omega,\beta)=\frac{1}{2\pi}\mathbf{P}_i(\omega)*W_r(\omega,\beta)=\frac{1}{2\pi}\int_{-\infty}^{\infty}\mathbf{P}_i(\tau)W_r(\omega-\tau,\beta)d\tau \tag{21}$$

where $\mathbf{P}_i(\omega)$and $W_r(\omega, \beta)$ can be written directly from Eq. (5), (5b) and (8), respectively:

$$\mathbf{P}_i(\omega)=k_{ts}t_x\begin{pmatrix}P_1(\omega)\\P_2(\omega)\\P_3(\omega)\end{pmatrix}=k_{ts}t_x\begin{pmatrix}\frac{j\pi}{2}[\delta(\omega+2)-\delta(\omega-2)]\\\pi\delta(\omega)-\frac{\pi}{2}[\delta(\omega+2)+\delta(\omega-2)]\\j\pi[\delta(\omega+1)-\delta(\omega-1)]\end{pmatrix} \tag{22}$$

$$\mathbf{P}_2(\omega)=k_{tp}\begin{pmatrix}P_4(\omega)\\P_5(\omega)\\P_6(\omega)\end{pmatrix}=k_{tp}\begin{pmatrix}\pi\left[\delta(\omega+1)+\delta(\omega-1)\right]\\j\pi\left[\delta(\omega+1)-\delta(\omega-1)\right]\\2\pi\delta(\omega)\end{pmatrix} \quad (22b)$$

and

$$W_r(\omega,\beta)=\frac{2\sin(\omega\frac{\theta_r}{2})}{\omega}e^{-j\omega\frac{\theta_1+\theta_2}{2}} \quad \text{with} \quad \theta_r=\theta_2(\beta)-\theta_1(\beta) \quad (23)$$

Substituting Eqs. (22), (22b) and (23), Eq. (21) becomes

$$\mathbf{P}_{1w}(\omega,\beta)=k_n t_x\begin{pmatrix}P_{1w}(\omega,\beta)\\P_{2w}(\omega,\beta)\\P_{3w}(\omega,\beta)\end{pmatrix}=k_n t_x\begin{pmatrix}\frac{j}{4}[W_r(\omega+2)-W_r(\omega-2)]\\\frac{1}{2}W_r(\omega)-\frac{1}{4}[W_r(\omega+2)+W_r(\omega-2)]\\\frac{j}{2}[W_r(\omega+1)-W_r(\omega-1)]\end{pmatrix} \quad (24)$$

$$\mathbf{P}_{2w}(\omega,\beta)=k_{tp}\begin{pmatrix}P_{4w}(\omega,\beta)\\P_{5w}(\omega,\beta)\\P_{6w}(\omega,\beta)\end{pmatrix}=k_{tp}\begin{pmatrix}\frac{1}{2}[W_r(\omega+1)+W_r(\omega-1)]\\\frac{j}{2}[W_r(\omega+1)-W_r(\omega-1)]\\W_r(\omega)\end{pmatrix} \quad (24b)$$

Equations (24) and (24b) are equivalently to Eqs. (19) and (19b) although they are expressed in a different way. $P_i(\omega)$'s in Eqs. (22) and (22b) are shown to be impulse functions defined only at discrete frequencies with ω=0, 1 or 2.

Equation (23) indicates that magnitude of $W_r(\omega, \beta)$ is a *sinc* function with periodic zeros starting at $\omega = 2\pi/\theta_r$ with a period of $2\pi/\theta_r$ and with a decaying envelope of $1/\omega$. The locations of local zeros are clearly shown to depend on the radial immersion angle, θ_r, and then the radial immersion angle can be chosen so that zeros of the frequency spectra fall on the integer frequencies with periods of 2, 3, 4… and so on, which can be used to suppress the harmonics of cutting force. If $\theta_r/2$ can be expressed in $(n_s/m_s)\pi$ where n_s/m_s is the simplest fraction, then the frequency spectra of $W_r(\omega)$ will have the zeros with period of m_s. Table 1 shows the special radial immersion angles corresponding to the zeros of the frequency spectra with periods of 2, 3, 4 and 5. It is noted that the zeros with period 5 is shared by both $\theta_r = 2\pi/5$ and $\theta_r = 4\pi/5$ due to the common m_s=5 for $\theta_r = 2\pi/5$ and $\theta_r = 4\pi/5$. Period of 2 correspond to the special case of slot milling. Except for slot milling, it should be noted that different radial depths of cut can still yield the same θ_r and consequently result in the same frequency spectra for $W_r(\omega)$ with different workpiece offset c shown in Figure 1.

Equations (24) and (24b) indicate that the frequency spectrum of each $P_{iw}(\omega)$ is simply the scaled sum of $W_r(\omega)$ sampled at one or the combination of these three frequencies: ω, $\omega \pm 1$ and $\omega \pm 2$. Since magnitude of $W_r(\omega)$ is a *sinc* function with periodic zeros, some elements of the $\mathbf{P}_{iw}(\omega)$'s will be reduced to zero at the harmonic frequencies $\omega=Nk$ if the periodic zeros of $W_r(\omega)$ fall on the integer frequencies of ω=1, 2, etc. This statement is illustrated in Table 2 showing the zeros of $\mathbf{P}_{iw}$'s for the same five radial immersion angles as in Table 1. Due to the specific radial immersion angles chosen in Table 1, zeros of Table 2 are also located at integer frequencies at ω=0, 2, 3, 4, etc., depending on each individual P_i.

Slot milling condition has closely spaced periodic zeros at ω=2, 4, 6,… in $W_r(\omega)$, and therefore results in significant number of zeros at integer frequencies in $\mathbf{P}_{iw}$ as shown in Table 2. These zeros have special significance in affecting the force spectra of a general helical end mill in slot milling. Since the entry and exit angles in slot milling are 0 and π, independent of β for any helical cutter, Eq. (17) can be reduced to Eq. (20) where shows the frequency characteristics of $\mathbf{P}_{iw}$ in slot milling have a direct multiplicative effect on the spectra of the total forces $\mathbf{F}_{1i}(\omega)$ regardless of the integration results and zeros of $\mathbf{P}_{iw}$'s are also zeros of $\mathbf{F}_{1i}(\omega)$. Therefore, from Table 2, the harmonic components of the shearing forces in the X-Y plane at ω=4, 6, 8… will vanish since the linear combination of P_1 and P_2 constitutes the X-Y plane component of the shearing forces. Similarly, the harmonic components of the ploughing force components in the X-Y plane will vanish at ω =3, 5, 7… since the linear combination of P_4 and P_5 constitutes the X-Y plane component of the ploughing forces. Since the harmonic frequencies of an N-flute cutter are at $\omega=Nk$, the shearing force pulsation will therefore completely vanish for a cutter of N=4, 6, 8.., and the odd-numbered harmonic components for the ploughing force as well as the even- numbered harmonic components for the shearing force will not exist for a cutter of N=3, 5, 7... In addition, for a two-flute cutter with general profile in slot milling, the dynamic shearing force components in the X-Y plane can possibly exist only at the first harmonic with ω=2, while the ploughing component in the X-Y plane can possibly exist at each harmonic.

Radial immersion	Frequency locations of zeros of $W_r(\omega)$
$\theta_r = \pi$	ω = 2, 4, 6,…, etc. (period of 2)
$\theta_r = 2\pi/3$	ω = 3, 6, 9,…, etc. (period of 3)
$\theta_r = \pi/2$	ω = 4, 8, 12,…, etc. (period of 4)
$\theta_r = 2\pi/5$	ω = 5, 10, 15,…, etc. (period of 5)
$\theta_r = 4\pi/5$	ω = 5, 10, 15,…, etc. (period of 5)

Table 1: Special radial immersion angles corresponding to frequency locations of zeros of $W_r(\omega)$ with periods of 2, 3, 4 and 5.

Radial immersion		Frequency locations of zeros
P_{1w}	$\theta_r = \pi$	ω = 4, 8, 12,…, etc.
	$\theta_r = \pi/2$	ω = 6, 12, 18,…, etc.
	$\theta_r = 2\pi/3,\ 2\pi/5$ and $4\pi/5$	None
P_{2w}	$\theta_r = \pi$	ω = 4, 8, 12,…, etc.
	$\theta_r = 2\pi/3,\ \pi/2,\ 2\pi/5$ and $4\pi/5$	None
P_{3w}	$\theta_r = \pi$	ω = 3, 5, 7,…, etc.
	$\theta_r = 2\pi/3,\ \pi/2,\ 2\pi/5$ and $4\pi/5$	None
P_{4w}	$\theta_r = \pi$	ω = 3, 5, 7,…, etc.
	$\theta_r = 2\pi/3,\ \pi/2,\ 2\pi/5$ and $4\pi/5$	None
P_{5w}	$\theta_r = \pi$	ω = 3, 5, 7,…, etc.
	$\theta_r = 2\pi/3,\ \pi/2,\ 2\pi/5$ and $4\pi/5$	None
P_{6w}	$\theta_r = \pi$	ω = 2, 4, 6,…, etc.
	$\theta_r = 2\pi/3$	ω = 3, 6, 9,…, etc.
	$\theta_r = \pi/2$	ω = 4, 8, 12,…, etc.
	$\theta_r = 2\pi/5$	ω = 5, 10, 15,…, etc.
	$\theta_r = 4\pi/5$	ω = 5, 10, 15,…, etc.

Table 2: Zeros of the frequency spectra of the windowed elemental force functions in $P_{1w}(\omega)$-$P_{6w}(\omega)$ under the same immersion angles as in Table 1.

The spectra characteristics mentioned above led to the suggestion that in order to reduce the force pulsation in the *X-Y* plane for rough machining, cutter with even-numbered flute (except for N=2) is recommended to use in slot milling as shearing force is dominated due to the aggressive feed rate. On the other hand, if ploughing force is dominated in slot milling, for example in finish machining with small feed per tooth, cutter with odd-numbered flute (except for N=1) is recommended to use, which can diminish the force pulsation in the *X-Y* plane effectively.

Equations (4-7) show that Z component of the milling forces is dependent only on $P_3(\omega)$ and $P_6(\omega)$ for the shearing and ploughing contributions respectively. Therefore, for cutter with N=2, 4, 6.., the dynamic component of the ploughing force in the Z direction vanishes, and for cutter with N=3, 5, 7.., the odd harmonics of the shearing components of the Z force will not exist. Therefore, the effects of flute number on the force spectra in the cutter axis direction are almost to the opposite of those in the *X-Y* plane, except that the dynamic ploughing force in Z direction completely disappears for N=2.

For a single flute cutter in slot milling, the frequency spectra of the shearing and ploughing components in the X, Y and Z directions can be directly inferred from Table 2 since their kth harmonics are determined by the spectra at each integer frequency $\omega=k$; they show a strong presence of the first and second harmonics except the second harmonic in P_6.

Although some of the above statement on the characteristics of the shearing and ploughing force components in slot milling has also been brought up from a different perspective and experimentally proved for a square end mill in ref. [23], these observations are shown here to also hold true for a milling cutter with a general helical profile.

Equation (20) also applies for half slot milling in either up or down cut configuration since the entry and exit angles are also independent of the cutting edge geometry. In either down or up cut, the Fourier transforms of W_r have the same magnitude and differ only in their phases. Both are characterized by the periodic zeros at ω=4, 8, 12...as shown in Table 1. From Table 2, it is clear that in half slot milling only $P_{1w}(\omega)$ will be zero at ω=6, 10, 14..and $P_{6w}(\omega)$ are zero at ω=4, 8, 12.. Therefore, neither the shearing nor ploughing components of the dynamic forces in the *X-Y* plane at any frequency $\omega=Nk$ will vanish completely in half slot milling for any type of milling cutter. However, for a cutter of N=4, 8, 12.., the ploughing force pulsation in the Z direction will completely vanish in half slot milling.

For other radial depths of cut with $\theta_r=2\pi/3$, $\theta_r=2\pi/5$ and $\theta_r=4\pi/5$, Table 2 shows that $\mathbf{P}_{iw}(\omega)$ will have zero only in $P_{6w}(\omega)$ at ω =3, 6… for $\theta_r=2\pi/3$, and have zero only in $P_{6w}(\omega)$ at ω=5, 10… for $\theta_r=2\pi/5$ and $\theta_r=4\pi/5$. This means that ploughing force components of the dynamic forces in the Z direction will vanish for a cutter of N=3, 6, 9… in milling with $\theta_r=2\pi/3$ and a cutter of N=5, 10, 15… in milling with $\theta_r=2\pi/5$ or $\theta_r=4\pi/5$. In fact, from Eq. (23) and the condition of periodic zeros, it can further be shown that neither shearing nor ploughing force components of the dynamic forces in the *X-Y* plane will vanish in a non-slot milling configuration for a general helical cutter of any flute number if only the spectra of $\mathbf{P}_{iw}(\omega)$'s are considered. However, it should be noted that, depending on the outcome of the integration in Eq. (17) or (20) which include the effects of $\mathbf{q}_i h'(\beta)$, harmonics components of the milling forces might not exist at $\omega=Nk$ even though they are predicted to exist according to the spectra of $\mathbf{P}_{iw}(\omega)$'s.

Calculating the Fourier Series Coefficients

Fourier coefficients not only allow analyzing the frequency spectra of the milling forces, but also provide an efficient way of synthesizing the angle or time domain forces through inverse Fourier transform. The evaluation of Fourier coefficients is equivalent to finding the values of the Fourier transform of Eq. (17) at $\omega=Nk$. However, a closed form expression of Eq. (17) generally does not exist for a general milling cutter in a general cutting configuration. The main obstacle to obtaining a closed form is that the entry and exit angles vary with the cutting point position along the cutting edge and $\mathbf{q}_i(\psi(\beta))h'(\beta)$ is generally complex transcendental function. However, as long as the analytical expressions for $\mathbf{q}_i(\psi(\beta))$, $h'(\beta)$ and the boundaries of the cutting region, $\theta_1(\beta)$, $\theta_1(\beta)$ and β_1, β_2,, can be obtained or their numerical values are available, Eqs. (16) and (17) can be evaluated using one of the two methods below.

Semi-analytic method

An algebraic semi-analytic equation can be obtained if the continuous integration in Eq. (17) is approximated by discrete summation in finite axial depth of cut or in finite interval of $\Delta\beta$. Hence, Eq. (14) can be approximated by:

$$\mathbf{F}_i(\omega) \cong \sum_{i=1}^{2}\sum_{m=0}^{M-1} \mathbf{q}_i(\beta_1+m\Delta\beta)\mathbf{P}_i(\omega,\beta_1+m\Delta\beta)h'(\beta_1+m\Delta\beta)e^{-j\omega(\beta_1+m\Delta\beta)}\Delta\beta \quad \text{with} \quad \Delta\beta=\frac{\beta_a}{M} \tag{25}$$

The summation approach of Eq. (25) lends itself to straight computer implementation. This semi-analytic method is different from obtaining the forces from the numerical integration of local cutting forces, where the cutting action of each cutting point is individually accounted for and the position of each cutting flute has to be kept track of in order to determine if cutting points are engaged in the cutting. Equation (25) thus provides a convenient means to obtain the approximated frequency spectra, whose accuracy is easily improved by using a finer $\Delta\beta$. Another attractive feature of Eq. (25) is that it does not require analytic expressions for the geometric functions, $\mathbf{q}_i(\beta)$, $h'(\beta)$, and $\mathbf{P}_{iw}(\omega, \beta)$. Therefore, discrete values of cutter/workpiece profile data given from scanning can be used to calculate the Fourier coefficients of the milling forces directly.

Numerical integration using general software package

If $\mathbf{q}_i(\beta)$, $h'(\beta)$ and $\mathbf{P}_{iw}(\omega,\beta)$ have analytical expressions, $\mathbf{F}_1(\omega)$ in Eq. (17) can be calculated using general numerical integration routine, such as QUAD or QUAD8 command in Matlab. This approach is similar in nature to that of the Eq. (25), however, requiring less programming work if one is proficient with the chosen software.

Conclusion

In a common framework, a space-time convolution approach has been presented to find the Fourier coefficients of milling force for general helical end mills with the shearing and ploughing cutting mechanisms. The angular domain total force is composed as a convolution integration of differential forces along the cutting edge for a single flute and the total forces are the sum of the periodically shifted single flute forces. The frequency domain force model is derived through Fourier transform and the Fourier coefficients of the total cutting forces are formulated as an analytical integral expression by the modified convolution theorem. The line geometry of the cutting edge, the number of flutes, the depths of cut, and cutting configuration have all been integrated into a single framework suitable for finding the Fourier coefficients of the milling forces and for investigating the effects of cutting parameters on the force spectra characteristics in a general milling operation.

It is shown that the flute number N completes the frequency domain model for the total milling forces by introducing a multiplying factor N for all the harmonics as well as the average forces and specifies

the harmonics frequencies at $\omega=Nk$. In slot milling, the shearing force components in the plane of feed will vanish for N=4, 6, 8.., while the odd harmonic components of the ploughing forces will vanish for N=3, 5, 7... However, for the force in the cutter axis direction, the effect of cutter flute number on the shearing and ploughing components is almost reversed. Based on the spectra characteristics, when slot milling is performed, cutters with even-numbered flute and odd-numbered flute (except for N=1) are recommended to use for rough machining and finish machining respectively in order to reduce the force pulsation in the X-Y plane. However, if the cutting force in the cutter axis direction is dominated, the strategy for selecting cutters is reversed.

The frequency spectra of a general helical cutter are shown to decrease in ω^{-2} yielding significant drop in magnitude of higher harmonics. The periodic milling forces of a general helical milling cutter in the continuous angular or time domain can therefore be simply and adequately represented by only a few Fourier coefficients in the discrete frequency domain. By virtue of the explicit expression of Fourier coefficients of milling force, this model provides a formulation to calculate the Fourier coefficients of the milling forces if the profile of cutter/workpiece can not be analytically definable and only the discrete geometrical data of a helical cutting edge and workpiece profile are given from scanning. When the cutting geometry of a helical cutting edge and workpiece profile can be analytically defined and then the Fourier coefficients of milling force can be simply calculated using general numerical integration routine, such as QUAD or QUAD8 command in Matlab.

It is believed that the present research will facilitate the transfer of experience on one type of cutter to another with greater ease. To this effect, the application of this frequency domain force model will be illustrated for three most common industrial cutters in the second part of this paper where the specific geometric functions and integrations boundaries required for the evaluation of Fourier coefficients will be presented and a closed form formula for the identification of six shearing and ploughing cutting constants will be derived.

Acknowledgement

The authors gratefully acknowledge the financial support from Quanzhou Institute of Information Engineering.

References

1. Smith S, Tlusty J (1991) An Overview of modeling and simulation of the milling process. ASME Journal of Engineering for Industry 113:169- 175.
2. Ehmann KF, Kapoor SG, DeVor RE, Lazoglu I (1997) Machining process modeling a review. ASME Journal of Manufacturing Science and Engineering 119: 655-663.
3. Koenigsberger F, Sabberwal AJP (1961) An Investigation into the Cutting Force Pulsations During Milling Operations. International Journal of Machine Tool Design and Research 1:15-33.
4. Tlusty J, MacNeil P (1975) Dynamics of cutting force in end milling. Annals of CIRP 24: 21-25.
5. Boothroyd G (1975) Fundamentals of Metal Machining and Machine Tools Scripta Book Co Washington DC.
6. Masuko M (1953) Fundamental research on metal cutting (1st report) a new analysis of cutting forces. Transaction of JSME 19: 32-39.
7. Yellowley I (1985) Observations on the mean values of forces torque and specific power in the peripheral milling process. International Journal of Machine Tool Design and Research 25: 337-346.
8. Armarego EJA, Whitfield RC (1985) Computer based modeling of popular machining operations for forces and power prediction. Annals of CIRP 34: 65-69.
9. Endres WJ, DeVor RE, Kapoor SG (1995)A Dual-Mechanism Approach to the Prediction of Machining Forces Part 1: Model Development and Part 2: Calibration and Validation. ASME Journal of Engineering for Industry 117: 526-541.
10. Budak E, Altintas Y, Armarego EJA (1998) Prediction of Milling Force Coefficients From Orthogonal Cutting Data. ASME Journal of Manufacturing Science and Engineering 118: 216-224.
11. Abrari F, Elbestawi MA (1997) Closed Form Formulation of Cutting Forces for Ball and Flat End Mills. International Journal of Machine Tools & Manufacture 27: 17-27.
12. Kline WA, DeVor RE, Lindberg JR (1982) The Prediction of Cutting Forces in End Milling with Application to Cornering Cuts. International Journal of Machine Tool Design and Research 22: 7-22.
13. Altintas Y, Lee P (1996) A General Mechanics and Dynamics Model for Helical End Mills. Annals of CIRP 45: 59-64.
14. Engin S, Altintas Y (2001) Mechanics and dynamics of general milling cutters Part I: helical end mills. International Journal of Machine Tools & Manufacture 41: 2195-2212.
15. Wan M, Zhang WH, Qin GH, Tan G (2007) Efficient calibration of instantaneous cutting force coefficients and runout parameters for general end mills. International Journal of Machine Tools & Manufacture 47: 1767-1776.
16. Sun Y, Guo Q (2011) Numerical simulation and prediction of cutting forces in five-axis milling processes with cutter run-out. International Journal of Machine Tools & Manufacture 51: 806-815.
17. Yellowley I (1988) A Note on the significance of the quasi-mean resultant force and the modelling of instantaneous torque and forces in peripheral milling. ASME Journal of Engineering for Industry 110: 300-303.
18. Yellowley I, Hosepyan Y, Oyawaye O (1992) The identification of machining conditions and tracking of tool wear in milling using machining forces. Material Issues in Machining and the Physics of Machining Processes, ASME Winter Annual Meeting: 111-130.
19. Seethaler RJ, Yellowley I (1999) The Identification of radial runout in milling operations. ASME Journal of Manufacturing Science and Engineering 121: 524-531.
20. Wang JJ, Liang SY, Book WJ (1994) Convolution analysis of milling force pulsation. ASME Journal of Engineering for Industry 116: 17-25.
21. Zheng L, Li Yawei, Liang SY (1997) A Generalized model of milling forces. International Journal of Advanced Manufacturing Technology 14: 160-171.
22. Lazoglu I, Liang SY (1997) Analytical modeling of ball-end milling force. Int. J. of Machining Science and Technology 1: 219-234.
23. Wang JJ, Zheng CM (2002) An analytical force model with shearing and ploughing mechanisms for end milling. International Journal of Machine Tools & Manufacture 42: 761-771.
24. Wang JJ, Zheng CM (2002) Identification of shearing and ploughing cutting constants from average forces in ball-end milling. International Journal of Machine Tools & Manufacture 42: 695-705.
25. Gygax PE (1975) Dynamics of single-tooth milling. Annals of CIRP 29: 61-66.
26. Oppenheim AV, Willsky AS, Young IT (1983) Signals and Systems Prentice-Hall Inc New Jersey.